Extraction of density-layered fluid from a porous medium

J. Jose[1] G. Hocking[2] D. Farrow[3]

(Received 8 January 2020; revised 20 June 2020)

Abstract

We consider axisymmetric flow towards a point sink from a stratified fluid in a vertically confined aquifer. We present two approaches to solve the equations of flow for the linear density gradient case. Firstly, a series method results in an eigenfunction expansion in Whittaker functions. The second method is a simple finite difference method. Comparison of the two methods verifies the finite difference method is accurate, so that more complicated nonlinear, density stratification can be considered. Such nonlinear profiles cannot be considered with the eigenfunction approach. Interesting results for the case where the density stratification changes from linear to almost two-layer are presented, showing that in the nonlinear case there are certain values of flow rate for which a steady solution does not occur.

DOI:10.21914/anziamj.v61i0.14996, Published 2020-07-07, as part of the Proceedings of the 14th Biennial Engineering Mathematics and Applications Conference. ISSN 1445-8810.

Contents

1 Introduction C138

2 Problem formulation C139

3 Linear density gradient C141
3.1 Series solutions C141
3.2 Finite difference solution C143

4 Nonlinear density gradient C145

5 Summary C148

References C149

1 Introduction

Flow of fluids in porous media is very important across a range of applications. Oil recovery from underground, pumping fresh water from aquifers and mineral leaching in mining applications are obvious examples [3]. A characteristic of the fluids in many of these applications is that they are stratified in density, either due to fluid properties (oil-water), salt content (fresh-water, salt-water) or temperature [6, 14, 7].

The basic law for the flow of fluids through porous media is Darcy's Law,

$$\mathbf{q} = -\frac{k}{\mu}\nabla\Phi\,, \tag{1}$$

where $\mathbf{q}$ is the specific discharge (velocity), k is the permeability of the porous medium, μ is the fluid viscosity, and the piezometric head is defined as

$$\Phi = \frac{p}{\hat{\rho}g} + z\,, \tag{2}$$

Figure 1: Sketch defining the variables for flow into a point sink located at $(0, d)$. Arrows indicate the direction of flow and $\hat{\rho}$ is the variable density gradient. The duct has total height d. The radial coordinate is r and the vertical coordinate is z.

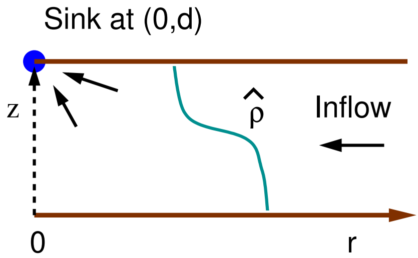

where $\hat{\rho}$ is the density, p is the pressure, g is gravity and z is the elevation head. Traditional solution methods [3, 11, 14, 13] include modelling the interface as a free boundary and simplifying the equations to those that can be solved quickly and accurately. The results of traditional methods provide good tests of simulation packages such as COMSOL [4], but also provide better understanding of the dynamic processes.

2 Problem formulation

Consider the axisymmetric flow of a stratified fluid into a point sink on the top surface of a vertically confined aquifer. In cylindrical coordinates the sink is situated at $r = 0$ and on the top of a vertically confined region with height d (see Figure 1.). The flow is assumed to be radially symmetric toward the sink, and the fluid to have a density stratification $\hat{\rho}(r, z)$.

Following the work of Yih [11], consider the cylindrical coordinates (r, ϕ, z) with z increasing vertically upward. In axisymmetric flow, the flow is independent of ϕ, and the pseudo-velocity is defined by

$$(u', w') = \frac{\mu}{\mu_0}(\hat{u}, \hat{w}), \tag{3}$$

where μ_0 is a constant reference viscosity, and $\hat{u}$ and $\hat{w}$ are the velocity components in the r and z directions, respectively. In terms of the pseudo-velocity, the equations of motion (1) become

$$\frac{\mu_0}{k} u' = -\frac{\partial p}{\partial r} \quad \text{and} \quad \frac{\mu_0}{k} w' = -\frac{\partial p}{\partial z} - g\hat{\rho} . \tag{4}$$

Since μ does not change along a streamline in steady flows, u' and w' satisfy the continuity equation and so we use a new stream function ψ' which is defined by

$$u' = -\frac{1}{r}\frac{\partial \psi'}{\partial z} \quad \text{and} \quad w' = \frac{1}{r}\frac{\partial \psi'}{\partial r} . \tag{5}$$

After some work [11] we reach the equation

$$\left(\frac{\partial^2}{\partial z^2} + \frac{\partial^2}{\partial r^2} - \frac{1}{r}\frac{\partial}{\partial r} \right) \psi' = -\frac{kgr}{\mu_0}\frac{d\hat{\rho}}{d\psi'}\frac{\partial \psi'}{\partial r} . \tag{6}$$

If the fluid is incompressible, then in steady flow $\hat{\rho}$ is a function of ψ' only.

We now solve (6) together with appropriate boundary conditions

$$\psi' = \begin{cases} 0, & r = 0\,, \quad 0 < z < d\,; \\ 0, & z = 0\,, \quad r > 0\,; \\ Q, & z = d\,, \quad r > 0\,; \end{cases} \tag{7}$$

where Q is the discharge into the sink. The discontinuity of ψ' at $r = 0$ and $z = d$ represents the sink.

Define the upstream $(r \to \infty)$ density as $\hat{\rho} \to f(z)$. To reduce the number of parameters in the problem, we use the dimensionless quantities

$$(\xi, \zeta) = \left(\frac{r}{d}, \frac{z}{d} \right), \quad \Psi = \frac{2\pi\psi'}{Q}, \quad \rho = \frac{\hat{\rho}}{\rho_0},$$

then (6) becomes

$$\left(\frac{\partial^2}{\partial \xi^2} - \frac{1}{\xi}\frac{\partial}{\partial \xi} + \frac{\partial^2}{\partial \zeta^2} \right) \Psi = \left(-\frac{2\pi kg\xi\rho_0}{Q\mu_0} \right) \frac{d\rho}{d\Psi}\frac{\partial \Psi}{\partial \xi} , \tag{8}$$

with the boundary conditions

$$\Psi = \begin{cases} 0, & \xi = 0\,, \quad 0 < \zeta < 1\,; \\ 0, & \zeta = 0\,, \quad \xi > 0\,; \\ 1, & \zeta = 1\,, \quad \xi > 0\,. \end{cases} \tag{9}$$

3 Linear density gradient

A long way upstream ($\xi \to \infty$) we assume a linear density gradient $\rho = 1 - \beta\zeta$, so that $\frac{d\rho}{d\zeta} = f'(\zeta) = -\beta$. For a linear gradient, a long way upstream $\Psi \to \zeta$ as the flow velocity approaches zero, and since in incompressible flow the density along a streamline remains the same, then it is true everywhere that

$$\frac{d\rho}{d\Psi} = -\beta\,.$$

The non-dimensional form of equation (6) with the linear density gradient is

$$\left(\frac{\partial^2}{\partial\xi^2} - \frac{1}{\xi}\frac{\partial}{\partial\xi} + \frac{\partial^2}{\partial\zeta^2}\right)\Psi = \left(\frac{2\pi k g \beta \rho_0 d}{Q\mu_0}\right)\xi\frac{\partial\Psi}{\partial\xi} = \lambda^2\xi\frac{\partial\Psi}{\partial\xi}\,, \tag{10}$$

where

$$\lambda^2 = \frac{2\pi k g \beta \rho_0 d}{Q\mu_0} \tag{11}$$

is proportional to the density gradient or the inverse of the flux Q. Thus, the problem is to solve (10) with the boundary conditions (9) along with $\Psi \to \zeta$ as $\xi \to \infty$.

3.1 Series solutions

Following Yih [11], and in accordance with boundary conditions (9), we seek a solution as an eigenfunction expansion in the form

$$\Psi = \zeta + \sum_{n=1}^{\infty} A_n g_n(\xi) \sin n\pi\zeta\,. \tag{12}$$

The differential equation satisfied by $g_n(\xi)$ is

$$g_n'' - \left(\lambda^2\xi + \frac{1}{\xi}\right) g_n' - n^2\pi^2 g_n = 0\,, \tag{13}$$

where $g_n(0) \neq 0$, and $g_n \to 0$ as $n \to \infty$.

The differential equation (13) has a regular singular point at $\xi = 0$ and so we use the Frobenius method in powers of ξ [15]. Following Yih [11] we let $g = e^{\frac{\eta}{2}} h(\eta)$ where $\eta = \frac{\lambda^2\xi^2}{2}$, and then we finally reach

$$h''(\eta) + \left(-\frac{1}{4} + \frac{k_n}{\eta}\right) h(\eta) = 0\,. \tag{14}$$

Equation (14) has solutions in the form of a Whittaker function [1], and the appropriate solution is

$$g_n(\xi) = \int_0^\infty t^{-k_n} \left(\frac{\lambda^2\xi^2}{2} + t\right)^{k_n} e^{-t}\,dt\,, \tag{15}$$

where

$$k_n = \frac{-n^2\pi^2}{2\lambda^2}\,.$$

At $\xi = 0$, $g_n(0) = 1$ from (15), and coefficients A_n are chosen to satisfy (9), so that the stream function

$$\Psi = \zeta + \sum_{n=1}^{\infty} \frac{2(-1)^n}{n\pi} g_n(\xi) \sin n\pi\zeta\,.$$

Streamlines for $\lambda = 1$ and $\lambda = 8$ are shown in Figure 2. For $\lambda = 1$, the flow is stronger nearer to the sink due to the higher flow rate, and so the streamlines 'fill' more of the channel. The flow coming from the bottom part of the duct is relatively slow when $\lambda = 8$ and so the streamlines fill less of the depth. This effect is clearly seen in the velocity profiles shown in Figure 3. For the case $\lambda = 8$ there is a region near the bottom of the aquifer that is almost stagnant.

Figure 2: Streamlines $\psi = 0, 0.1, \ldots, 1$ of a stratified fluid flow due to a point sink with $\lambda = 1$ (left) and $\lambda = 8$ (right). Larger λ indicates lower flow rate, so at higher flow the streamlines fill more of the channel.

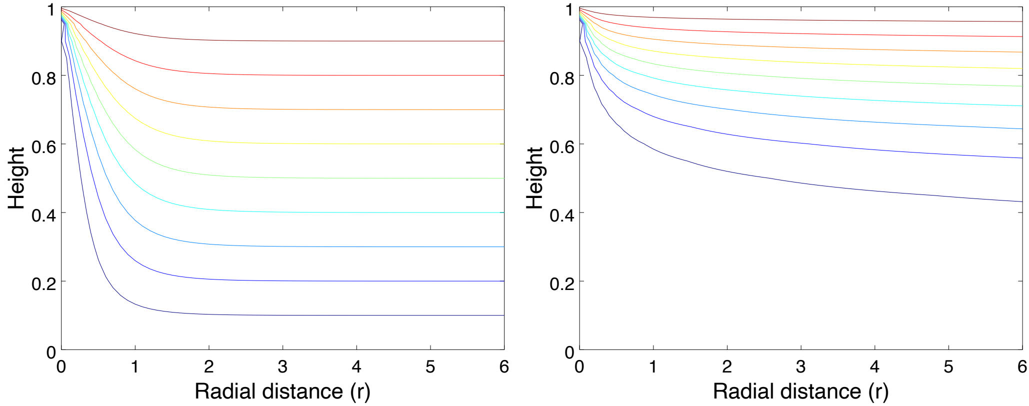

3.2 Finite difference solution

To compute solutions for flows in which the density stratification is not linear we approach the problem using the finite difference method. First we compare the solution with that computed by Yih [11] for the case of a linear density gradient, presented in Section 3.1, and then we consider a case in which the density gradient is not linear. In particular we are interested in the case with two layers of different density.

If we make a guess for $\Psi(\xi, \zeta)$, at the grid points (ξ_i, ζ_j), $i = 2, 3, \ldots, N-1$ and $j = 2, 3, \ldots, M-1$, separated by $\Delta\xi$ and $\Delta\zeta$, respectively, then the errors at the corresponding points for the finite difference form of (10) are

$$\begin{aligned} E_{i,j} = {} & \Psi_{i+1,j}\left[\Delta\zeta^2 - \frac{1}{2}\left(\frac{1}{\xi_i} + \lambda^2\xi_i\right)\Delta\xi\Delta\zeta^2\right] + \Psi_{i,j}\left(-2\Delta\xi^2 - 2\Delta\xi^2\right) \\ & + \Psi_{i-1,j}\left[\Delta\zeta^2 + \frac{1}{2}\left(\frac{1}{\xi_i} + \lambda^2\xi_i\right)\Delta\xi\Delta\zeta^2\right] + \Psi_{i,j+1}\Delta\xi^2 + \Psi_{i,j-1}\Delta\xi^2 \,, \\ & i = 2, \ldots, N-1\,, \quad j = 2, \ldots, M-1\,. \end{aligned}$$

Figure 3: Velocity profiles in the duct at locations $\xi = 0.75, 1, 1.5, 3$ (left to right curves in each plot). Here the dots represents the eigenfunction solution and the lines represent the finite difference solutions with $\lambda = 1$ (left) and $\lambda = 8$ (right). At the lower flow rate ($\lambda = 8$), flow is faster in a narrow layer at the level of the sink.

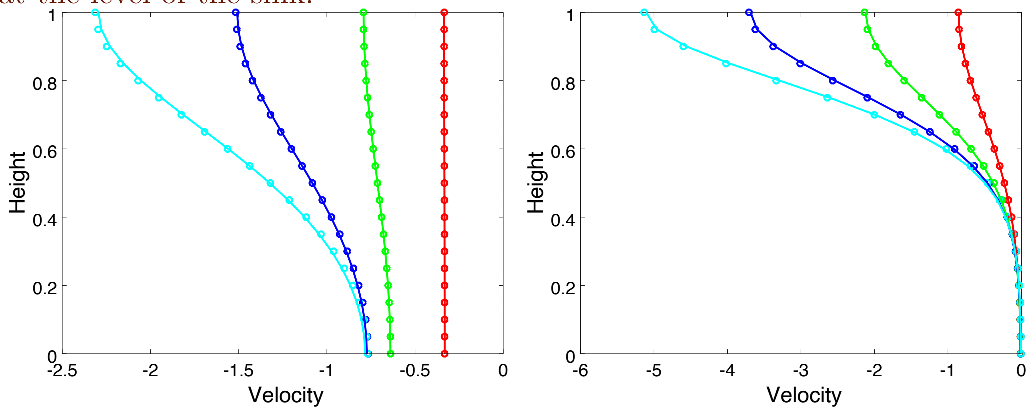

The values of $\Psi_{i,1}$, $\Psi_{i,M}$ and $\Psi_{1,j}$ are given by the boundary conditions (9). This gives $(M-2) \times (N-2)$ equations in the same number of unknowns which can be solved in Octave [10] using the nonlinear equation solver `fsolve`. Solutions were computed using $\lambda = 1, 8$ for comparison with the series solutions. The contours (not shown) are very similar to those shown in Figure 2 and the comparative velocity profiles of the two cases are given in Figure 3 with good agreement.

Now that we have verified the finite difference method we consider different density strata. In particular, we are interested in the behaviour as the linear gradient transitions into a two-layer strata with a region of lighter fluid sitting on top of a region of heavier fluid.

Figure 4: The nonlinear density profiles for different densities $d_2 = 0.4\pi$ (left) and $d_2 = 0.49\pi$ (right). This is a typical density profile for stratified fluid as used by Farrow and Hocking [5].

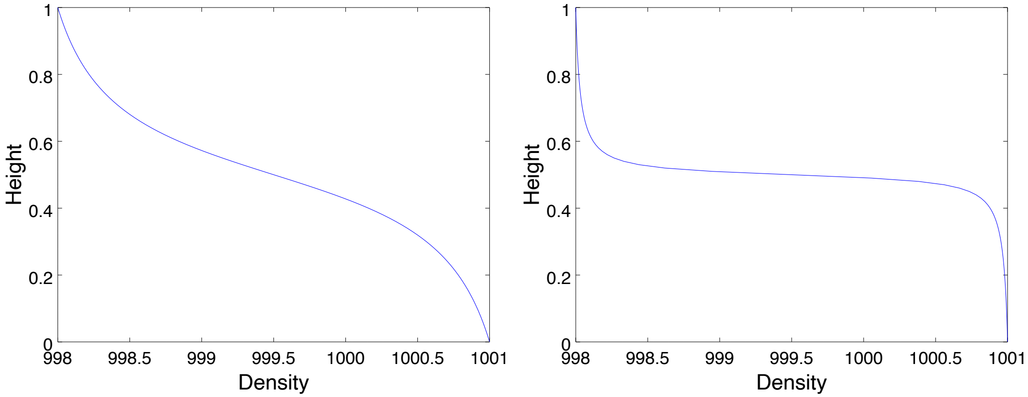

4 Nonlinear density gradient

In order to consider the case of general stratification of the form $\rho(\zeta) = f(\zeta)$, we use the density profile considered by Farrow and Hocking [5]

$$\rho = 1 + \frac{\frac{\rho_1}{\rho_0} - 1}{2d_2} \left(\arctan\left[d_1(2\zeta - 1)\right] + d_2\right), \tag{16}$$

where ρ_0, ρ_1 are densities at the top and bottom, respectively, and $\rho_0 < \rho_1$. The values of d_1 and d_2 determine the shape of the density profile, as seen in Figure 4, and are related by the expression $d_1 = \arctan(d_2)$.

In the upstream limit $\xi \to \infty$, $\Psi \to f(\zeta)$. After differentiating ρ with respect to Ψ we obtain

$$\frac{\partial\rho}{\partial\Psi} = \left(\frac{\rho_1}{\rho_0} - 1\right) \frac{d_1}{d_2} \frac{1}{\left[1 + d_1(2\Psi - 1)\right]^2}. \tag{17}$$

Substituting (17) into (6) we find

$$\frac{\partial^2\Psi}{\partial\xi^2} - \left(\frac{1}{\xi} - G^2\xi f(\Psi)\right) \frac{\partial\Psi}{\partial\xi} + \frac{\partial^2\Psi}{\partial\zeta^2} = 0, \tag{18}$$

Figure 5: The streamlines $\psi = 0, 0.1, \ldots, 1$ for $G = 1$ (left) and $G = 8$ (right) with density profile value $d_2 = 0.4\pi$. Stronger flow has smaller G. These correspond to the density profile in the left panel of Figure 4.

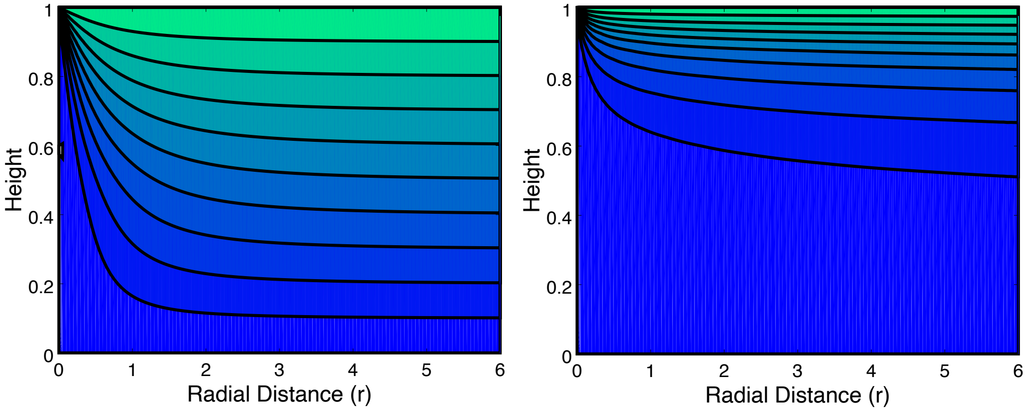

where $G^2 = \lambda^2/\beta$. We now treat equation (18) as a boundary value problem with the boundary conditions (7) plus $\frac{d\Psi}{d\xi} \to 0$ as $\xi \to \infty$ and $0 < \zeta < 1$, and solve using the finite difference method.

For lower G, discharge into the sink is very high, while for higher G, discharge into the sink is low. Figure 5 shows the streamlines of the flow with density stratification for $d_2 = 0.4\pi$, for a high flow case $G = 1$ and a low flow case $G = 8$. As in the case of the linear density gradient, the flow remains stronger over the full depth of the duct when the flow is stronger. This is emphasized by Figure 6 which shows the velocity in the top layer is moving relatively quickly towards the point sink, while the bottom layer is almost stagnant. This effect is much stronger for the lower flow rate $G = 8$. Figure 7 shows the velocity profiles for the stratification in which $d_2 = 0.49\pi$. The stronger density layering exaggerates the velocity layering effect. In Figure 8 the density contours are shown for the gradient with $d_2 = 0.4\pi$, and this shows that when $G = 1$ the interface in the middle of the two layers is simply pulled up in the vicinity of the sink, but for $G = 8$ the flow is not strong enough to sustain a flow over the whole layer and overcome the density gradient, so the

Figure 6: Velocity profiles at locations, $\xi = 0.75, 1, 1.5, 3$ (left to right curves in each plot) with density profile $d_2 = 0.4\pi$, and $G = 1$ (left) indicates the strong flow and $G = 8$ (right) indicates the weak flow. The weaker flow starts to exhibit a strong two-layer velocity structure.

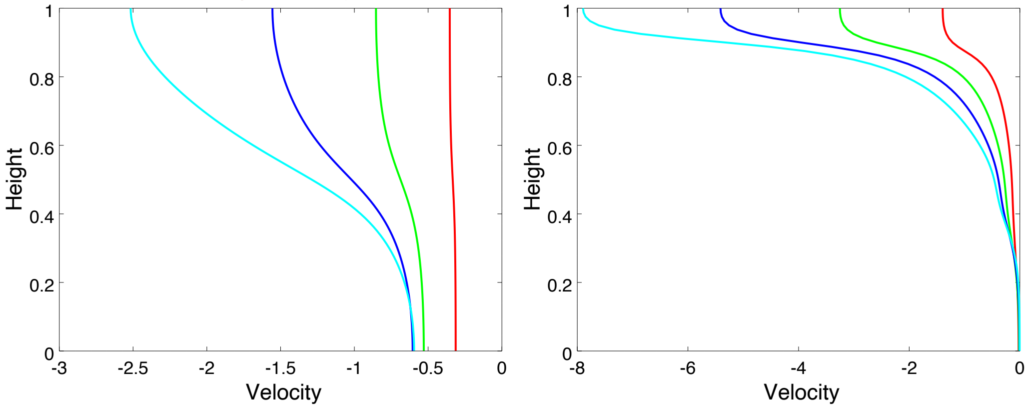

Figure 7: Velocity profiles at locations, $\xi = 0.75, 1, 1.5, 3$ (left to right curves in each plot) with $G = 1$ and with different densities obtained from $d_2 = 0.4\pi$ (left) and $d_2 = 0.49\pi$ (right). The sharper density step ($d_2 = 0.49\pi$) leads to a distinct step in the velocity profile and lower velocity in the bottom layer.

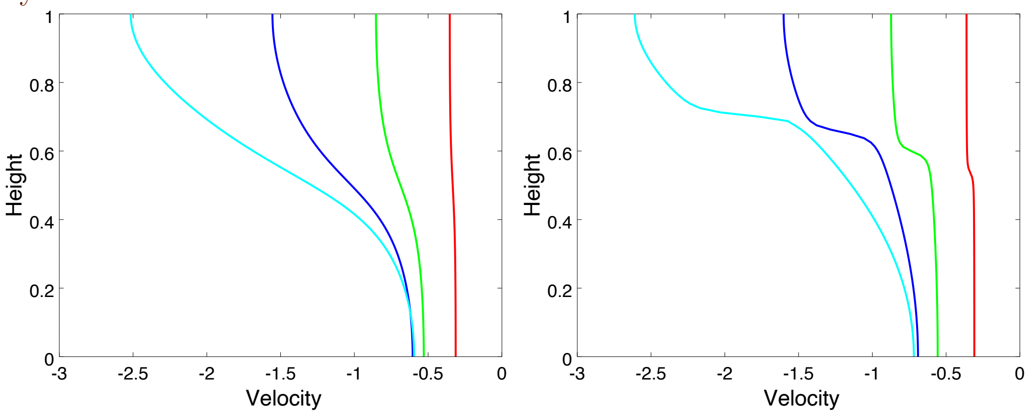

Figure 8: Density contours $\rho = 999, 999.5, 1000$ for $d_2 = 0.4\pi$ with $G = 1$ (left), which shows a high flow rate and water flowing over the whole depth, and $G = 8$ (right), which shows a narrow layer develops near the top.

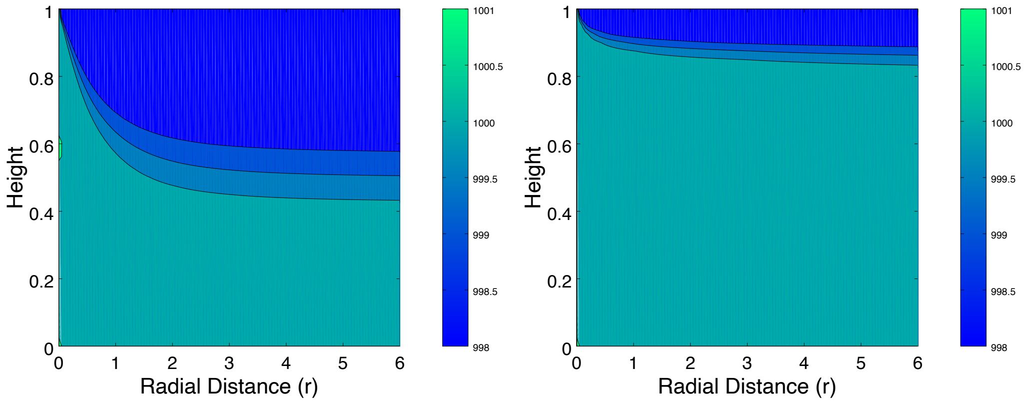

fluid flows in a very narrow layer near the level of the sink. This indicates that there is no valid solution for an initial profile with the mid-point of density at $\zeta = 0.5$ and so there is no steady solution for this upstream condition when G is greater than some value that depends on the flow rate and the stratification.

5 Summary

We have considered axisymmetric flow of a stratified fluid into a point sink in a vertically confined aquifer. First we considered the case where the density stratification was linear. Two methods of solution were used. Following Yih [11] a separation of variables approach led to an eigenfunction expansion in Whittaker functions, and then a finite difference method was used. A comparison showed good agreement between the two methods, verifying the numerical approach.

The eigenfunction expansion method cannot be used for a more complicated nonlinear stratification in which the density gradient is not a constant, and so the finite difference method was extended so that we could consider any density gradient. Velocity profiles were plotted to understand the effects of variations in flow rate and in density. We also identified the differences for nonlinear density profiles and found regions where no steady solutions seem to exist for some upstream density profiles and flow rates. Changing the location of the point sink and considering fluids with a very sharp interface are the next steps in this study.

References

[1] Abramowitz, M. and Stegun, I. A., *Handbook of Mathematical Functions*, 9th ed. National Bureau of Standards, Washington, 1972. C142

[2] Bear, J. and Dagan, G. "Some exact solutions of interface problems by means of the hodograph method". *J. Geophys. Res.* 69(8):1563–1572, 1964. doi:10.1029/JZ069i008p01563

[3] Bear, J. "Dynamics of fluids in porous media". Elsevier, New York, 1972. `https://store.doverpublications.com/0486656756.html` C138, C139

[4] COMSOL Multiphysics. "COMSOL Multiphysics Programming Reference Manual", version 5.3. `https://doc.comsol.com/5.3/doc/com.comsol.help.comsol/COMSOL_ProgrammingReferenceManual.pdf` C139

[5] Farrow, D. E. and Hocking, G. C. "A numerical model for withdrawal from a two layer fluid". *J. Fluid Mech.* 549:141–157, 2006. doi:10.1017/S0022112005007561 C145

[6] Henderson, N., Flores, E., Sampaio, M., Freitas, L. and Platt, G. M. "Supercritical fluid flow in porous media: modelling and simulation". *Chem. Eng. Sci.* 60:1797–1808, 2005. doi:10.1016/j.ces.2004.11.012 C138

[7] Lucas, S. K., Blake, J. R. and Kucera, A. "A boundary-integral method applied to water coning in oil reservoirs". *ANZIAM J.* 32(3):261–283, 1991. doi:10.1017/S0334270000006858 C138

[8] Meyer, H. I. and Garder, A. O. "Mechanics of two immiscible fluids in porous media". *J. Appl. Phys.*, 25:1400–1406, 1954. doi:10.1063/1.1721576

[9] Muskat, M. and Wycokoff, R. D. "An approximate theory of water coning in oil production". *Trans. AIME* 114:144–163, 1935. doi:10.2118/935144-G

[10] GNU Octave. https://www.gnu.org/software/octave/doc/v4.2.1/ C144

[11] Yih, C. S. "On steady stratified flows in porous media". *Quart. J. Appl. Maths.* 40(2):219–230, 1982. doi:10.1090/qam/666676 C139, C140, C141, C142, C143, C148

[12] Yu, D., Jackson, K. and Harmon, T. C. "Disperson and diffusion in porous media under supercritical conditions". *Chem. Eng. Sci.* 54:357–367, 1999. doi:10.1016/S0009-2509(98)00271-1

[13] Zhang, H. and Hocking, G. C. "Axisymmetric flow in an oil reservoir of finite depth caused by a point sink above an oil-water interface". *J. Eng. Math.* 32:365–376, 1997. doi:10.1023/A:1004227232732 C139

[14] Zhang, H., Hocking, G. C. and Seymour, B. "Critical and supercritical withdrawal from a two-layer fluid through a line sink in a bounded aquifer". *Adv. Water Res.* 32:1703–1710, 2009. doi:10.1016/j.advwatres.2009.09.002 C138, C139

[15] Zill, D. G. and Wright, W. S. *Differential Equations with Boundary-value problems*, 8th Edition. Brooks Cole, Boston USA, 2013. C142

Author addresses

1. **J. Jose**, Mathematics and Statistics, Murdoch University, Murdoch, WA, 6150 Australia.
   mailto:jyothijose2011@gmail.com
   orcid:0000-0002-2093-4594
2. **G. Hocking**, Mathematics and Statistics, Murdoch University, Murdoch, WA, 6150 Australia.
   mailto:g.hocking@murdoch.edu.au
   orcid:0000-0002-5812-6015
3. **D. Farrow**, Mathematics and Statistics, Murdoch University, Murdoch, WA, 6150 Australia.
   mailto:d.farrow@murdoch.edu.au
   orcid:0000-0002-4716-7698